Beyond mean field model for Gamow-Teller giant resonances and β decay

M. J. YANG(1), C. L. BAI(1), H. SAGAWA(2)(3)(*) and H. Q. ZHANG(4)

(1) *College of Physics, Sichuan University - Chendu 610065, China*
(2) *RIKEN, Nishina Center - Wako 351-0198, Japan*
(3) *Center for Mathematics and Physics, University of Aizu - Aizu-Wakamatsu, Fukushima 965-8560, Japan*
(4) *China Institute of Atomic Energy - Beijing 102413, China*

Summary. — The Gamow-Teller (GT) transitions in four magic nuclei ^{48}Ca, ^{90}Zr, ^{132}Sn, and ^{208}Pb are studied by self-consistent Hartree-Fock (HF) plus charge-exchange subtracted second random phase approximation (SSRPA) model with several Skyrme energy density functions (EDFs). These calculations show that SSRPA improves systematically the description of main GT strength distributions in terms of the excitation energy and the peak height. The quenching factors are evaluated to be 13-20% of the Ikeda sum rule for ^{48}Ca, ^{90}Zr, and ^{132}Sn, due to the couplings to two particle-two hole (2p-2h) configurations. The effect of tensor interaction on the β decay half-life in SSRPA model is also pointed out to change largely the half-lives by about one to two orders of magnitude with respect to the ones obtained without tensor force.

1. – Introduction

The theoretical studies of giant resonances in nuclei have made successful progress in the last two decades. Particularly, the microscopic models, such as HF+random phase approximation (RPA), which based on the self-consistent mean-field approximation with the EDFs, are intensively developed in these years. However, the RPA model including only one particle-one hole (1p-1h) configurations cannot provide good account of the spreading width due to the coupling to the many-particle many-hole configurations [1-4]. Moreover, in the GT transitions, a large quenching of the sum rule value was found experimentally in the giant GT excitation energy region lower than 20 MeV [5].

The nuclear β decay is a weak interaction process, which plays a significant role in the neutron capture process of stellar nucleosynthesis [6,7]. The β decay rates set the

---

(*) Corresponding author. E-mail: hiroyuki.sagawa@gmail.com

time scale of the rapid neutron capture process (r-process), which is responsible for the synthesis of half of the nuclei heavier than iron and all heavy actinide nuclei.

In this work, the self-consistent HF+SSRPA calculations based on the Skyrme EDFs are applied for the GT excitations of four closed shell nuclei ^{48}Ca, ^{90}Zr, ^{132}Sn, and ^{208}Pb to study the systematic trend of SSRPA on the description of GT strength distributions with respect to the excitation energy and the width. We will apply also the SSRPA model including tensor force to the β decay half-lives in magic and semi-magic nuclei, ^{34}Si, ^{68,78}Ni and ^{132}Sn with Skyrme EDFs.

2. – SSRPA and tensor interactions

In the SSRPA, we solve the secular equation including explicitly the $1p$-$1h$ and $2p$-$2h$ configurations. The detailed formalism was already discussed in several references (see for examples, refs. [8-10]), we will not provide it in this proceedings. The operator for GT transition is defined as

$$(1) \qquad \hat{O}_{GT}^{\pm} = \sum_{i=1}^{A} \sigma(i) t_{\pm}(i),$$

where σ is the spin operator and $t_{\pm} = t_x \pm i t_y$ are the isospin raising and lowering operators, respectively. The corresponding GT strength is defined as, $B_{1_n^+}^{GT^{\pm}} = |\langle 1_n^+ || \hat{O}_{GT}^{\pm} || 0 \rangle|^2$, where $|1_n^+\rangle$ is the n-th $J^{\pi} = 1^+$ state. The total GT strength obeys the model independent Ikeda sum rule [11],

$$(2) \qquad S_- - S_+ = \sum_n |\langle 1_n^+ || \hat{O}_{GT}^- || 0 \rangle|^2 - \sum_n |\langle 1_n^+ || \hat{O}_{GT}^+ || 0 \rangle|^2. = 3(N - Z)$$

The quenching factor for the transition strength in our discussion is defined with respect to the Ikeda sum rule. In present calculations, the triplet-even and triplet-odd zero-range tensor terms of the Skyrme force are introduced as

$$(3) \qquad v_T = \frac{T}{2} \left\{ \left[(\sigma_1 \cdot \mathbf{k}') (\sigma_2 \cdot \mathbf{k}') - \frac{1}{3} (\sigma_1 \cdot \sigma_2) \mathbf{k}'^2 \right] \delta(\mathbf{r}_1 - \mathbf{r}_2) \right.$$

$$+ \delta(\mathbf{r}_1 - \mathbf{r}_2) \left[(\sigma_1 \cdot \mathbf{k}) (\sigma_2 \cdot \mathbf{k}) - \frac{1}{3} (\sigma_1 \cdot \sigma_2) \mathbf{k}^2 \right] \right\}$$

$$+ U \left\{ (\sigma_1 \cdot \mathbf{k}') \delta(\mathbf{r_1} - \mathbf{r_2}) (\sigma_1 \cdot \mathbf{k}) - \frac{1}{3} (\sigma_1 \cdot \sigma_2) \mathbf{k}' \cdot \delta(\mathbf{r_1} - \mathbf{r_2}) \mathbf{k} \right\},$$

and thier roles are examined on GT and β decays.

3. – Gamow-Teller transitions and tensor forces

Figure 1 shows the strength distributions calculated with the SAMi-T EDF with or without tensor terms in RPA and SSRPA models [22]. The red and blue lines represent the calculations without and with tensor force, respectively. As shown in this figure, in RPA calculations without the tensor force, the excitation energies of the main peaks appear about 1-2 MeV higher in energy than those with the tensor force in all nuclei. In SSRPA calculations, the tensor force shifts the main peaks downwards by about 1 to 1.5
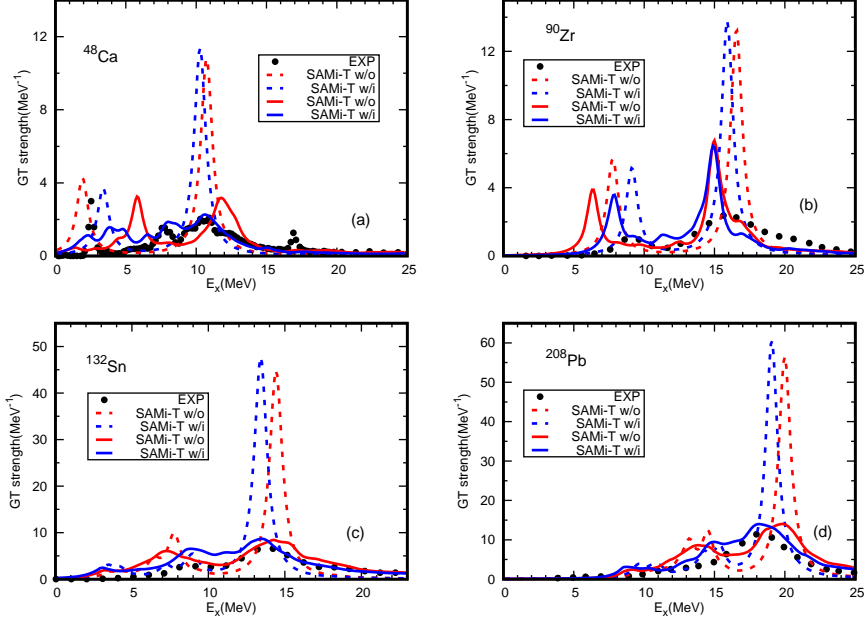
Fig. 1. – GT$_-$ strength distributions of ^{48}Ca [panel (a)], ^{90}Zr [panel (b)], ^{132}Sn [panel (c)] and ^{208}Pb [panel (d)] calculated with the SAMi-T EDF with or without tensor terms. Red lines represent SAMi-T without tensor terms labeled w/o, and blue lines represent the SAMi-T EDF with tensor terms labeled w/i. The dashed lines show the RPA results, while the solid lines are SSRPA ones. The experimental data of ^{48}Ca [12],^{90}Zr [13], ^{132}Sn [14], and ^{208}Pb [15] are shown by the black filled circles. The calculated discrete strength distributions are convoluted by a Lorentzian weighting function of 1 MeV width. See the text for more details.

MeV and the peak heights are reduced, and becomes almost the same as the experimental ones in ^{48}Ca, ^{132}Sn, and ^{208}Pb. Particularly, in ^{48}Ca, the including of the tensor terms reproduces well not only the main peak at Ex=11 MeV, but also the shoulder at around Ex=7.5 MeV. We can see also better descriptions of main peaks in ^{132}Sn and ^{208}Pb in terms of the excitation energy and the peak heights. On the other hand, in ^{90}Zr, the excitation energy of the main peak is almost unchanged by the tensor force, and the agreement with the experimental data is modest.

The corresponding cumulative sums are shown in fig. 2. The SSRPA calculations show gradual increase of the sum until Ex=15 MeV similar trend to the experimental ones, while those of RPA show abrupt increase at the main GT peak energies. The quenching factors obtained by SSRPA model give just few percent changes after including tensor terms. This might be due to the week strength of the tensor force in SAMi-T.

The quenching factors, which corresponds to the percentage of the strength shifted to the high energy region, for the four nuclei ^{48}Ca, ^{90}Zr, ^{132}Sn and ^{208}Pb together with the strength of tensor force of SAMi, SAMi-T, SGII, SGII+Te1, SGII+Te2, and SGII+Te3 are listed in table I. In general, the tensor interactions give more quenching than those without the tensor force ones. One interesting point to observe from the table is that the SGII+Te1 and SGII+Te3 with the triplet-odd tensor U term give more quenching
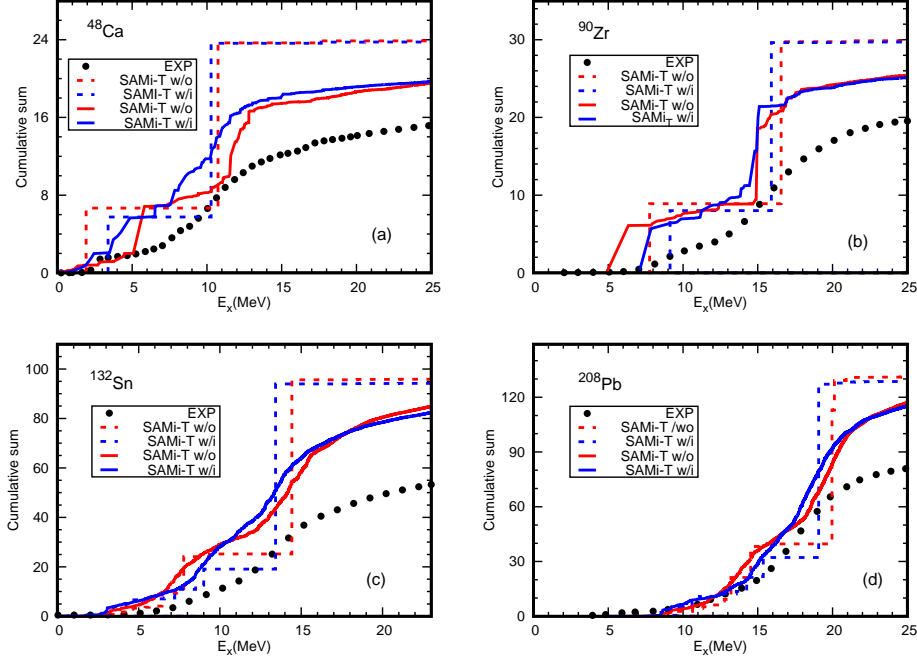
Fig. 2. – Cumulative GT$_-$ strengths up to 25 MeV for ^{48}Ca [panel (a)] and ^{90}Zr [panel (b)], 23 MeV for ^{132}Sn [panel (c)], and 25 MeV for ^{208}Pb [panel (d)] calculated with for the SAMi-T EDF with or without tensor terms. Red lines represent SAMi-T without tensor terms labeled w/o, blue lines represent SAMi-T with tensor terms labeled w/i. SGII and SAMi The results are given by RPA (dash lines) and SSRPA (solid lines). The experimental data of ^{48}Ca [12],^{90}Zr [13], ^{132}Sn [14], and ^{208}Pb [15] are shown by the black filled circles.

than the one without U term. Especially, the quenching factors calculated with the SGII+Te1 EDF are systematically increased by about 10% in comparison with the SGII EDF in the four nuclei. This indicates that the tensor forces with stronger strengths give larger quenching factors, being close to the experimental data and consistent with the calculated results in ref. [16].

In the above calculations the J^2 terms are included in both HF and SSRPA, but in the original SGII they were not included in the HF level. Because of this reason, we perform calculations in which the J^2 terms from the momentum dependent part of the Skyrme interactions are excluded in both HF and SSRPA for SGII. The results are labeled by SGII^O in order to distinguish from the ones with J^2 terms. Figure 3 shows the strength distributions and corresponding cumulative sums of ^{48}Ca, ^{90}Zr, ^{132}Sn, and ^{208}Pb calculated with SGII^O, SGII^O+Te1, SGII^O+Te2, and SGII^O+Te3. Compared with the results with all the J^2 terms, those in fig. 3 reduce substantially the strengths of main peaks in all nuclei, as can be seen also in the quenching factors in table I. The results of SGII^O irrespective to the tensor interactions give additional 10∼20 % quenching in table I. In the strength distributions, SGII^O EDF without tensor terms reproduce well the main peaks of ^{48}Ca and ^{90}Zr, but not so good for those of ^{132}Sn and ^{208}Pb. On the other hand, SGII^O+Te2 and SGII^O+Te3 give good accounts of main peaks of ^{132}Sn
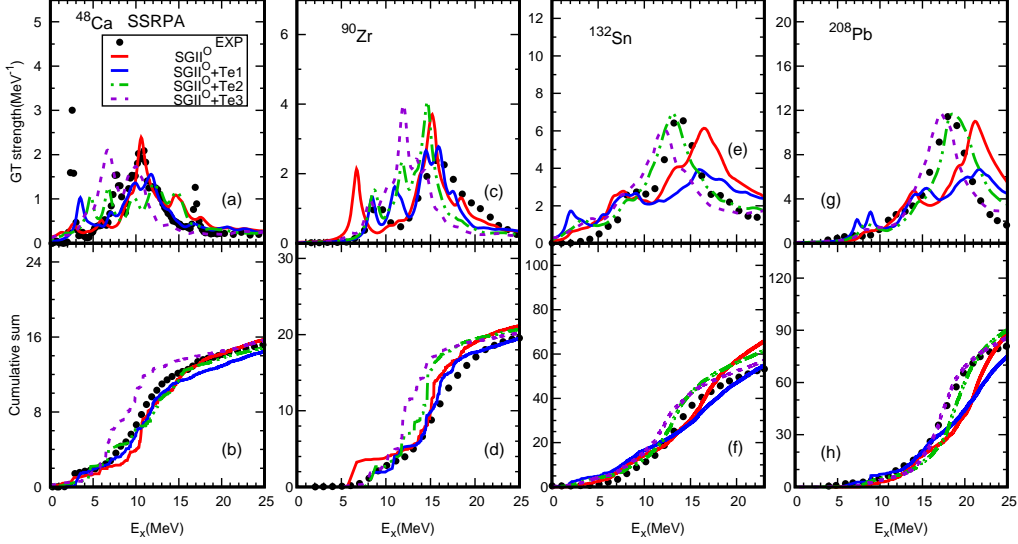
Fig. 3. – Strength distributions [upper panels] and corresponding cumulative sums [lower panels] of ^{48}Ca [panel (a), (b)], ^{90}Zr [panel (c), (d)], ^{132}Sn [panel (e), (f)] and ^{208}Pb [panel (g), (h)] calculated with SGII neglecting J^2 terms from the central interactions both in HF and SSRPA, and the results are labeled by SGII^O, SGII^O+Te1, SGII^O+Te2, and SGII^O+Te3, respectively.

and ^{208}Pb, but underestimate the peak energy of ^{90}Zr. Thus, SGII^O EDFs have an advantage to give a large quenching factor, especially, SGII^O+Te1 EDF. However, there is no improvement to describe the peak energies systematically compared with those obtained SGII EDFs with all the J^2 terms.

4. – β decay and tensor interactions

With the GT states calculated by the HF+SSRPA calculations, the GT-type β decay half-life can be calculated using a formula [19]:

$$(4) \qquad T_{1/2} = \frac{D}{g_A^2 \sum_n B_{1_n^+}^{GT^-} f_0(Z, A, \omega_n)},$$

where $D = 6163.4 \pm 3.8$ s (e.g., see ref. [20]), $f_0(Z, A, \omega_n)$ is the integrated phase factor, ω_n is the excitation energy of n-th GT state calculated being referred to the ground state of mother nucleus, and $g_A \equiv G_A/G_V = 1.26$ is the ratio of the axial-vector and vector coupling constants. The value g_A is usually set to lower than 1.26 assuming a quenching factor which is closely related to the GT sum rule deficiency [21]. In this work, the value

TABLE I. – *The quenching factor calculated by SSRPA with SAMi, SAMI-T, SGII, SGII+Te1, SGII+Te2, SGII+Te3, SGII^O, SGII^O+Te1, SGII^O+Te2, and SGII^O+Te3 EDFs. The strengths of tensor terms are also given. The cumulative sums are taken up to E_{max}=25 MeV for ^{48}Ca and ^{90}Zr, 23 MeV for ^{132}Sn, and 25MeV for ^{208}Pb in consistent with those of fig. 3.*

Force	(T,U)	^{48}Ca	^{90}Zr	^{132}Sn	^{208}Pb
SAMi	(0,0)	14.4%	15.2%	12.5%	10.0%
SAMi-T	(415.5,-95.5)	18.6%	16.3%	14.2%	12.7%
SGII	(0,0)	20.7%	19.2%	16.4%	14.7%
SGII+Te1	(500,-350)	28.7%	26.6%	28.7%	27.3%
SGII+Te2	(600, 0)	23.8%	22.1%	23.3%	19.0%
SGII+Te3	(650,200)	22.9%	24.1%	27.6%	23.6%
SGII^O	(0,0)	34.4%	29.4%	31.4%	33.2%
SGII^O+Te1	(500,-350)	39.8%	35.0%	42.8%	43.2%
SGII^O+Te2	(600, 0)	37.9%	31.0%	35.8%	31.7%
SGII^O+Te3	(650,200)	34.8%	32.6%	40.6%	35.0%
Exp.		36.7 %	34.9 %	44.5%	38.6 %

g_A is set to be $g_A = 1.0$. This value is consistent to the quenching factor in our previous work on the study of GT transition strengths by SSRPA model [22]. The sum about n runs over all 1^+ states within the β decay energy window $Q = \Delta_{nH} - \omega_n > 0$ MeV, with $\Delta_{nH} = 0.78227$ MeV denoting the mass difference between the neutron and hydrogen atom. When the energy is referred to the ground state of the daughter nucleus, the excitation energy is defined as $E_n = \omega_n - \Delta B$, where $\Delta B = B(Z, N) - B(Z+1, N-1)$ is the experimental binding energy difference of mother and daughter nuclei. This choice is convenient, because the calculated energy of the final 1^+ states can be directly compared to the experimental spectrum of the final nucleus. Then the upper limit of integration in eq. (4) becomes equal to the value $Q_\beta = \Delta_{nH} - \Delta B$, which is the experimental energy of β decay. When all the GT states are above the Q_β window, the nucleus is stable.

We study first the effect of the 2p-2h correlations taken into accounted in SSRPA model on the β-decay half-live of the four semi-magic and magic nuclei ^{132}Sn, ^{68}Ni, ^{34}Si, and ^{78}Ni [25]. Figure 4 shows the β decay half-lives calculated by RPA and SSRPA models, in comparison with experimental values. The RPA results largely overestimate the half-lives for almost all nuclei. Nuclei becomes artificially stable in RPA calculations such as ^{132}Sn, and the half-lives are infinite and not shown in this figure. On the other hand, the half-lives of all nuclei calculated with SSRPA become finite values, and become close to the experimental values. In the case of ^{68}Ni, we can see some discrepancies between the results of SSRPA and the experiments. In fig. 4, the SSRPA results of EDFs SLy5 and SkM* give better agreements of the half-lives in the four nuclei than the other EFDs in comparisons with the experimental data. Similar results were obtained by RPA+PVC calculations [24].

5. – Summary

In summary, we studied the GT transitions in four magic nuclei ^{48}Ca, ^{90}Zr, ^{132}Sn and ^{208}Pb by self-consistent HF+SSRPA model with different Skyrme EDFs. The SSRPA
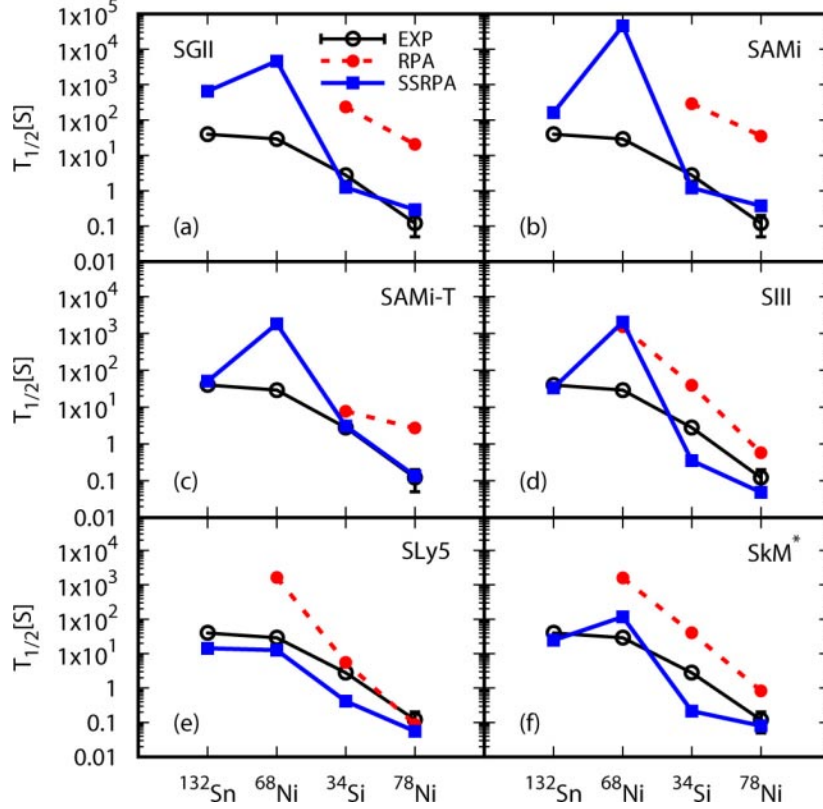
Fig. 4. – The β decay half-lives of ^{132}Sn, ^{68}Ni, ^{34}Si, and ^{78}Ni calculated by RPA and SSRPA models, respectively, in comparisons with experimental values [23]. The red solid circles and the blue solid squares represent results obtained by RPA and SSRPA respectively. The experimental data are shown by the black empty circles. The RPA results are infinite in some nuclei and not shown in the figure.

model describes systematically and quantitatively the GT strength distributions in the four nuclei better than the RPA model. Particularly the SGII and SAMi-T EDFs reproduce well the strength distributions of the main GT peaks in terms of the excitation energy and the peak height in comparison with the experimental data. We examined the effect of tensor terms in the SAMi-T EDF and found that they shift the main peaks downwards by about 1 MeV in ^{48}Ca, ^{132}Sn, and ^{208}Pb, but almost no effect in ^{90}Zr. The quenching factor are increased by about few percent, but these values with the tensor interactions are still about a half of the experimental quenching factors. We explored the possibility whether the tensor force with different strengths increases further or not the quenching factor of GT strength. To this end, we adopted the parameter sets SGII+Te1, SGII+Te2, and SGII+Te3. With these parameter sets, we found that the tensor interactions show strong effect on the spreading of the strength distribution, and shift of the excitation energy. As SGII is optimized excluding J^2 terms, we did the calculations in which the J^2 terms are excluded in both HF and SSRPA for SGII EDF. The calculations show that the exclusion of J^2 terms of the momentum dependent interactions gives larger quenching factors, close to experimental data.

We studied the half-lives of β decay in four magic and semi-magic nuclei ^{132}Sn, ^{68}Ni, ^{34}Si, and ^{78}Ni, using the self-consistent HF+SSRPA model with different Skyrme EDFs. In RPA calculations, the calculated half-lives are much longer than experiments and become infinite in ^{132}Sn an ^{68}Ni. The inclusion of 2p-2h configurations in SSRPA model in general can reduce systematically the lifetimes of β decay in the four nuclei. Particularly, it accelerates the β decay rates of ^{34}Si and ^{78}Ni by about two order of magnitude, and also produces finite half-lives for long-living nuclei ^{132}Sn and ^{68}Ni.

The effects of the tensor force in SSRPA are studied with the two EDFs SAMi-T and SGII+T. In SAMi-T, the tensor force accelerates the the β decay rates of ^{132}Sn and ^{68}Ni by about 5 times, while it increase the half-life of ^{34}Si largely. In the case of SGII+T with (T,U)=(500,-280) in ref. [25], the effect of tensor force is mainly observed in ^{68}Ni, in which the decay rate is accelerated by about two order of magnitude.

$$* \ * \ *$$

REFERENCES

[1] SPETH J. and VAN DER WOUDE A., *Rep. Prog. Phys.*, **44** (1981) 719.
[2] VAN DER WOUDE A., *Prog. Part. Nucl. Phys.*, **18** (1987) 217.
[3] AIT-TAHAR S. and BRINK D., *Nucl. Phys. A*, **560** (1993) 765.
[4] DROŻDŻ S., NISHIZAKI S., SPETH J. and WAMBACH J., *Phys. Rep.*, **197** (1990) 1.
[5] RAPAPORT J. *et al.*, *Nucl. Phys. A*, **410** (1983) 371.
[6] GROTZ K. and KLAPDOR H. V., *The Weak Interaction in Nuclear, Particle and Astrophysics* (Adam Hilger, Bristol) 1990.
[7] LANGANKE K. and MARTÍNEZ-PINEDO G., *Rev. Mod. Phys.*, **75** (2003) 819.
[8] GAMBACURTA D., GRASSO M. and ENGEL J., *Phys. Rev. Lett.*, **125** (2020) 212501.
[9] GAMBACURTA D., GRASSO M. and ENGEL J., *Phys. Rev. C*, **92** (2015) 034303.
[10] YANG M. J., BAI C. L., SAGAWA H. and ZHANG H. Q., *Phys. Rev. C*, **103** (2021) 054308.
[11] IKEDA K., FUJITA S. and FUJITA J. I., *Phys. Lett.*, **3** (1963) 271.
[12] YAKO K. *et al.*, *Phys. Rev. Lett.*, **103** (2009) 012503.
[13] WAKASA T. *et al.*, *Phys. Rev. C*, **55** (1997) 2909.
[14] YASUDA J. *et al.*, *Phys. Rev. Lett.*, **121** (2018) 132501.
[15] WAKASA T. *et al.*, *Phys. Rev. C*, **85** (2012) 064606.
[16] BERTSCH G .F. and HAMAMOTO I., *Phys. Rev. C*, **26** (1982) 1323.
[17] BAI C. L., SAGAWA H., ZHANG H. Q., ZHANG X. Z., COLÒ G. and XU F. R., *Phys. Lett. B*, **675** (2009) 28.
[18] BAI C. L., ZHANG H. Q., ZHANG X. Z., XU F. R., SAGAWA H. and COLÒ G., *Phys. Rev. C*, **79** (2009) 041301(R).
[19] ENGEL J., BENDER M., DOBACZEWSKI J., NAZAREWICZ W. and SURMAN R., *Phys. Rev. C*, **60** (1999) 014302.
[20] BORZOV I. N. and GORIELY S., *Phys. Rev. C*, **62** (2000) 035501.
[21] CAURIER E., MARTÍNEZ-PINEDO G., NOWACK F., POVES A. and ZUKER A. P., *Rev. Mod. Phys.*, **77** (2005) 427.
[22] YANG M. J., BAI C. L., SAGAWA H. and ZHANG H. Q., *Phys. Rev. C*, **106** (2022) 014319.
[23] http://www.nndc.bnl.gov.
[24] NIU Y. F., NIU Z. M., COLÒ G. and VIGEZZI E., *Phys. Rev. Lett.*, **114** (2015) 142501.
[25] YANG M. J., BAI C. L., SAGAWA H. and ZHANG H. Q., *Phys. Rev. C*, **107** (2023) 014325.